Effects of proton irradiation on the photoelectronic properties of microcrystalline silicon

Rudi Brüggemann, Stephan Brehme, Jean-Paul Kleider, Marie-Estelle Gueunier, Wolfgang Bronner

Effects of proton irradiation on the photoelectronic properties of microcrystalline silicon

R. Brüggemann [a,*], S. Brehme [b], J.P. Kleider [c], M.E. Gueunier [c], W. Bronner [d]

[a] *Institut für Physik, Carl von Ossietzky Universität Oldenburg, D-26111 Oldenburg, Germany*
[b] *Hahn-Meitner-Institut Berlin, Kekuléstr. 5, D-12489 Berlin, Germany*
[c] *Laboratoire de Génie Electrique de Paris (CNRS, UMR 8507), Supélec, Universités Paris VI et Paris XI, Plateau de Moulon, F-91192 Gif-sur-Yvette cedex, France*
[d] *2. Physikalisches Institut, Universität Stuttgart, Pfaffenwaldring 57, 70569 Stuttgart, Germany*

We report on proton irradiation of microcrystalline silicon with 2 MeV protons and find a drop in the mobility–lifetime product related to an increase in the density of gap states as revealed by modulated photocurrent experiments. The dark conductivity also drops due to a shift in the Fermi energy by defect creation and re-balance of charge. The impact on the ambipolar diffusion length, representing the minority-carrier properties, is much smaller. The electronic properties of P and B doped samples are hardly affected. We discuss the implications for microcrystalline silicon pin solar cells.

1. Introduction

The effects of irradiation of microcrystalline silicon (μc-Si:H) by photons or energetic particles like electrons and protons is of both fundamental and practical interest. It is of fundamental interest because any increase in defect density allows to study influence of defects on transport and recombination in this semiconductor. The practical interest stems from application in photovoltaics. Microcrystalline silicon has become an established semiconductor for photovoltaic and optoelectronic applications [1,2]. In combination with hydrogenated amorphous silicon (a-Si:H) it can be used in thin film tandem solar cells in the bottom-layer structure.

In addition to the favourable absorption coefficient for absorption in the infrared spectral region, and despite some metastability effects, μc-Si:H has been shown to exhibit no or insignificant degradation of the majority and minority carrier properties under light-soaking [3]. This is a main advantage over a-Si:H, which is known for years to suffer from light-induced degradation. In contrast to photon illumination, electron irradiation with 1-MeV electrons induces pronounced changes in the optical and electronic properties of microcrystalline silicon [4,5]. Upon electron irradiation, Ref. [5] reports an increase in sub-gap absorption as measured by the constant photocurrent method (CPM) and a deterioration of the photoconductive properties for both the majority and minority carriers, determined from steady-state photoconductivity (SSPC) and the steady-state photocarrier grating (SSPG) technique.

We have extended these irradiation experiments to study the effects of proton irradiation on μc-Si:H. This paper presents results for undoped and doped μc-Si:H samples on glass. These kinds of films are incorporated in the layered structure of μc-Si:H pin solar cells and diodes and individual layers have thus been studied. Microcrystalline silicon pin solar cells have shown a drop in efficiency upon proton irradiation [6].

High-energy protons above 100 MeV did not show any effect upon the optical and electronic properties in μc-Si:H [7]. Here, we investigate the effect of irradiation with 2-MeV protons, which have a larger damage

* Corresponding author. Tel.: +49-44 1798 3497; fax: +49-44 1798 3201.
E-mail address: rudi.brueggemann@uni-oldenburg.de (R. Brüggemann).

impact than 100-MeV protons, and we report changes in the photoelectronic properties and the density of states (DOS).

2. Experimental

Undoped microcrystalline silicon samples were deposited on Corning 7059 glass by plasma-enhanced chemical vapour deposition (PECVD) at 66 MHz excitation frequency [8] and hot-wire chemical vapour deposition (HWCVD) at a nominal substrate temperature of 300 °C [3]. The crystalline volume fraction estimated from the Raman spectra of these samples is about 75%. The actual crystalline volume fraction is larger as Raman spectra underestimate crystalline contributions to Raman scattering [4]. Doped μc-Si:H samples were taken from a doping series of HWCVD μc-Si:H samples, deposited at 400 °C [9].

Coplanar electrodes were evaporated on to the samples for the current measurements. We applied dark current, SSPC, SSPG and modulated photocurrent (MPC) and CPM measurements both before and after proton irradiation. We deduce the mobility–lifetime $\mu\tau$ products of the majority carriers from SSPC and the minority-carrier diffusion length L_d from SSPG. MPC [10,11] provided information on the density-of-states profile. The sub-gap absorption coefficient was determined by the constant-photocurrent method. For the P and B doped samples only the dark current, due to its high values, was measured before and after irradiation.

Proton irradiation was performed at room temperature with 2 MeV protons and a dose of 3×10^{13} cm^{-2}.

3. Results

Fig. 1 shows the temperature-dependent dark (I_d) and photocurrent (I_{ph}) of the PECVD μc-Si:H sample before and after proton irradiation. The photocurrent was measured under red illumination at a wavelength of 660 nm and at photon fluxes Φ of 10^{14} and 10^{15} cm^{-2} s^{-1}. The full symbols for the dark current indicate its drop after irradiation. This drop is associated with an increase in the activation energy E_a from 0.4 eV before to 0.56 eV after irradiation. The conductivity pre-factor σ_0 of $\sigma_d = \sigma_0 \exp(-E_a/kT)$ from the extrapolation of the conductivity σ_d to $1/T = 0$ does not change much and stays around 100 Ω^{-1} cm^{-1}. The photocurrent drops after irradiation in the whole temperature range. Comparing the diamond symbols with the circle symbols we note that this drop is lesser in magnitude at lower T.

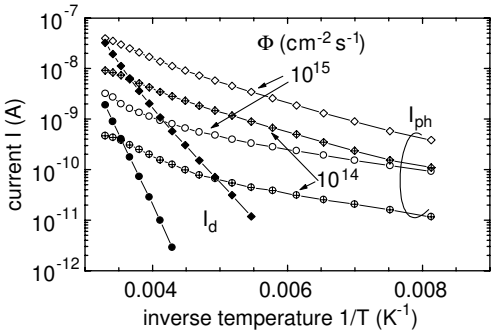

Fig. 1. Change in the temperature-dependent dark (full symbols) and photocurrent of the PECVD μc-Si:H sample before and after proton irradiation. The diamond (circle) symbols show the data before (after) irradiation. The photocurrent was measured at photon fluxes of 10^{14} and 10^{15} cm^{-2} s^{-1}.

Fig. 2 puts the $\mu\tau$ products of the irradiated samples into relation to those of a number of μc-Si:H samples from different deposition systems. The figure displays room-temperature $\mu\tau$ products for a photon flux of 10^{14} cm^{-2} s^{-1} of samples from Ecole Polytechnique [3] and Universität Stuttgart [8]. Data reported by Reynolds et al. [12] of samples from Forschungszentrum Jülich have also been included. The figure shows that the $\mu\tau$ products have the tendency to increase with increase in dark conductivity. The line is a guide for the eye. The increase in $\mu\tau$ product with shift of the Fermi level towards the conduction band, is typically found for a-Si:H [13–16] and also for μc-Si:H [17–19]. The irradiated samples fall well into the typical variation of $\mu\tau$ with σ_d before irradiation (upper full symbols). The two arrows indicate the decrease in $\mu\tau$ and σ_d upon proton irradiation.

Further effects of the 2-MeV proton irradiation on the properties of the unirradiated samples are summarized in Table 1. Here the B and P doped samples which have a dark conductivity σ_d between 0.1 and 1 Ω^{-1} cm^{-1} before irradiation are also included.

No significant effect of irradiation is found for the doped samples for which about the same dark conductivity is found before and after proton irradiation.

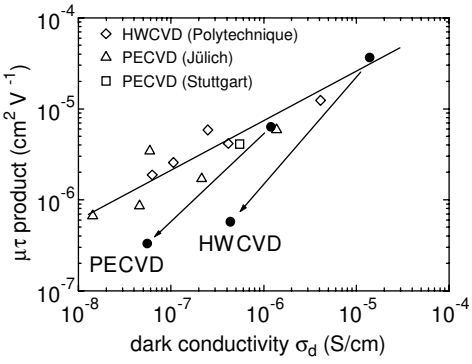

Fig. 2. Mobility–lifetime products vs. dark conductivity for the two irradiated undoped PECVD and HWCVD samples together with number of samples from different deposition systems. The line is a guide to the eye, indicating the increase in $\mu\tau$ with increase in σ_d. The arrows indicate the decrease in $\mu\tau$ and σ_d upon irradiation. Note that the slopes of the arrows are larger than for the straight line.

Table 1
Summary of changes in transport and electronic properties in μc-Si:H samples after proton irradiation at room temperature with 2-MeV protons. The data were measured at room temperature. The display in the format 'before/after', means 'measured before and after irradiation'; other variables mean: P – PECVD; H – HWCVD; (P) – P doped; (B) – B doped; (u) – undoped

Sample	σ_d (Ω^{-1} cm^{-1})	$\mu\tau$ (cm^2 V^{-1})	L_d (nm)
P (u)	$2.8\times10^{-7}/5\times10^{-8}$	$1.1\times10^{-7}/3.3\times10^{-8}$	164/140
H (u)	$2.7\times10^{-5}/2.5\times10^{-6}$	$2.5\times10^{-7}/5\times10^{-8}$	139/138
H (P)	0.41/0.33	–	–
H (B)	1/0.71	–	–

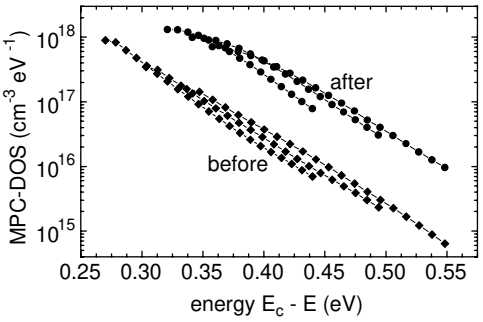

Fig. 3. MPC-DOS for the undoped HWCVD sample before and after proton irradiation. The MPC data were taken at three different temperatures (303, 273, 243 K), respectively, from which the MPC-DOS was pieced together with an attempt-to-escape frequency of 10^{11} s^{-1} and a mobility of 10 cm^2 V^{-1} s^{-1}.

For the undoped samples, Table 1 gives the mobility–lifetime products and the diffusion lengths determined from SSPC and SSPG experiments at $\Phi = 10^{17}$ cm^{-2} s^{-1}. At this higher photon flux the irradiation results in a drop in $\mu\tau$ which is smaller as compared to the results in Fig. 2, taken at the lower photon flux. The minority-carrier L_d is only slightly affected.

The ratio of the sub-gap CPM signal R_S, defined by $R_S = S^{after}_{CPM}/S^{before}_{CPM}$, where S_{CPM} is the calibrated CPM signal taken at 0.8 eV before and after proton irradiation, was also determined. The value of R_S is smaller than 3, respectively, for the undoped samples.

The MPC results obtained from modulated photocurrent phase and amplitude at a bias photon flux of 10^{14} cm^{-2} s^{-1} in Fig. 3 reflect the increase in the density-of-states (DOS) upon irradiation.

4. Discussion

The different results show a change in the electronic properties of the undoped μc-Si:H samples upon 2-MeV proton irradiation. In contrast and under the given irradiation conditions, the P and B doped HWCVD samples are stable, maintaining a high conductivity. As indicated by photodeflection spectroscopy on the doped samples, not shown here, these two samples show a high defect density in the as-deposited state which is not altered significantly by irradiation.

For the undoped samples we observe a drop in the dark conductivity after proton irradiation together with an increase in the dark-conductivity activation energy. A similar behaviour was reported after electron irradiation of undoped μc-Si:H [5,20]. The drop in dark conductivity can be understood in terms of a change of the Fermi level with the increase in the density of gap states. The Fermi level shifts as the newly created states require a redistribution of charge for the charge neutrality.

The two arrows in Fig. 2 indicate the drop in $\mu\tau$ and σ_d upon irradiation. Although a drop in $\mu\tau$ with decrease in σ_d can be anticipated, the decrease in $\mu\tau$ upon irradiation is larger and the data fall below the typical range, exhibiting an additional decrease in $\mu\tau$ than would be expected from the σ_d variation alone. The drop of the photocurrent after proton irradiation thus reflects the irradiation-induced increase in number of recombination states in the band gap for which we also find evidence from the DOS determination by the MPC experiments reported in Fig. 3. Although there is a clear increase in the MPC-DOS there are indications that its energetic distribution may not represent the true DOS when the scanned energy range is close to the Fermi or quasi-Fermi energy [21]. Taking the activation energy for the sample in Fig. 3 as a measure for the Fermi energy it is possible that the true DOS is larger, respectively.

While the SSPC and MPC techniques indicate the creation of additional recombination centres upon proton irradiation, they cannot provide further information on the microscopic nature of these irradiation-induced defects. To identify the silicon dangling bond as the defect that gets created upon proton irradiation, one can apply experiments like electron spin resonance (ESR) and electrically-detected ESR that have been useful for studying defect physics after electron irradiation [4,20].

The minority-carrier holes benefit from the Fermi level move closer to the valence band upon irradiation. Even though defects are created by proton irradiation, the diffusion length can be maintained close to the value as before irradiation. The related hole mobility–lifetime product, proportional to the square of the diffusion length, decreases lesser than the electron mobility–lifetime product. The hardly detectable change in the CPM signal after irradiation indicates that the gap state density below midgap is not altered to such an extent as the

density in the upper half of the gap, detected by MPC. This asymmetry in defect creation may also lead to the difference in irradiation induced changes of the electron and hole photoelectronic properties.

One may conclude that for proton irradiation in pin solar cell structures defect creation in the intrinsic layer will be mainly responsible for poorer excess carrier collection and thus poorer photovoltaic properties as the doped layers maintain their high dark conductivity, i.e., their Fermi-level positions. The shift of E_f in the undoped layers is beneficial for the minority-carrier properties which become less affected by the increased defect density. This effect also helps in the solar-cell minority-carrier collection after proton irradiation of these devices.

5. Conclusions

By proton irradiation of undoped μc-Si:H with 2-MeV protons and a dose of 3×10^{13} cm^{-2} at room temperature, the density of gap states in μc-Si:H increases which deteriorates the photoelectronic properties. Re-balance of charge is required in conjunction with a shift of the Fermi level, which decreases the dark conductivity and increases the dark-conductivity activation energy. Under the same irradiation conditions, doped samples appear to be stable in terms of dark conductivity values. From these film studies we thus suggest that the device performance for μc-Si:H solar cells exposed to proton irradiation will be mainly affected by the undoped μc-Si:H absorber layer rather than by irradiation-induced changes in the doped layers.

Acknowledgements

The authors thank H. Brummack, H.N. Wanka, Universität Stuttgart, and J. Guillet and J.E. Bourée, Ecole Polytechnique, Palaiseau, for providing samples. They also thank F. Jehn, Universität Jena, for the proton irradiation.

References

[1] A. Shah, Thin Solid Films 403&404 (2002) 179.
[2] O. Vetterl, F. Finger, R. Carius, P. Hapke, L. Houben, O. Kluth, A. Lambertz, A. Mück, B. Rech, H. Wagner, Solar Energy Mater. Cells 62 (2000) 97.
[3] R. Brüggemann, J.P. Kleider, C. Longeaud, D. Mencaraglia, J. Guillet, J.E. Bourée, C. Niikura, J. Non-Cryst. Solids 266–269 (2000) 258.
[4] F. Finger, J. Müller, R. Carius, C. Malten, in: J.M. Marshall, N. Kirov, A. Vavrek, J.M. Maud (Eds.), Thin Film Materials and Devices – Developments in Science and Technology, World Scientific, Singapore, 1999, p. 149.
[5] R. Brüggemann, W. Bronner, M. Mehring, Solid State Commun. 119 (2001) 23.
[6] J. Kuendig, M. Goetz, J. Meier, P. Torres, L. Feitknecht, P. Pernet, X. Niquille, A. Shah, L. Gerlach, E. Fernandez, in: H. Scheer et al. (Eds.), Proceedings of the 16th European Photovoltaic Solar Energy Conference, Glasgow, UK, May 2000, James & James Scient., London, 2000, p. 986.
[7] R. Brüggemann, J.P. Kleider, W. Bronner, I. Zrinscak, J. Non-Cryst. Solids 299–302 (2002) 632.
[8] H. Brummack, H.N. Wanka, A. Hierzenberger, R. Brüggemann, M.B. Schubert, Conference Record26th IEEE Photovoltaic Specialists Conference, Anaheim, 1997, IEEE, New York, 1997, p. 679.
[9] H. Wanka, R. Zedlitz, M. Heintze, M.B. Schubert, in: W. Freiesleben, W. Palz, H.A. Ossenbrink, P. Helm (Eds.), Proceedings of the 13th European Photovoltaic Solar Energy Conference, H.S. Stephens and Associates, Bedford, UK, 1995, p. 1753.
[10] R. Brüggemann, C. Main, J. Berkin, S. Reynolds,, Philos. Mag. 62 (1990) 29.
[11] J.P. Kleider, C. Longeaud, Solid State Phen. 44–46 (1995) 597.
[12] S. Reynolds, V. Smirnov, C. Main, R. Carius, F. Finger, MRS Symp. Proc. 715 (2002) A21.2.
[13] D.A. Anderson, W.E. Spear, Philos. Mag. 36 (1997) 695.
[14] P.E. Vanier, Sol. Cells 9 (1983) 85.
[15] W. Beyer, B. Hoheisel, Solid State Commun. 47 (1983) 573.
[16] J. Kočka, C.E. Nebel, C.-D. Abel, Philos. Mag. B 63 (1991) 221.
[17] H.N. Wanka, R. Brüggemann, C. Köhler, I. Zrinscak, M.B. Schubert, MRS Symp. Proc. 507 (1998) 915.
[18] R. Brüggemann, W. Bronner, A. Hierzenberger,, M.B. Schubert, I. Zrinscak, in: J.M. Marshall, N. Kirov, A. Vavrek, J.M. Maud (Eds.), Thin Film Materials and Devices – Developments in Science and Technology, World Scientific, Singapore, 1999, p. 1.
[19] F. Finger, S. Klein, T. Dylla, A.L. Baia Neto, O. Vetterl, R. Carius, Mater. Res. Soc. Symp. Proc. 715 (2002) A16.3.
[20] W. Bronner, M. Mehring, R. Brüggemann, Phys. Rev. B 16 (2002) 165212.
[21] R. Brüggemann, J.P. Kleider, Thin Solid Films 403 (2002) 30.